Stress-strain Laws for Carbon Black and Silicon Filled Elastomers

H.T. Banks and Laura K. Potter
(htbanks@eos.ncsu.edu, lkpotter@eos.ncsu.edu)
Center for Research in Scientific Computation
North Carolina State University
Raleigh, NC 27695-8205

Yue Zhang
CTA/PE3/E, Michelin North America Research Center
Greenville, SC 29605

November 24, 1997

Abstract

In this note we present results for nonlinear and hysteretic constitutive laws for filled elastomers. Theoretical, computational and experimental results are given.

1 Introduction

Filled rubber materials are widely used in today's industries due to their increased stiffness and wear-ability in comparison to their natural (unfilled) forms. They can be found traditionally in engine mounts, shock absorbers, automotive and aircraft parts (e.g., helicopter rotor dampers). Newly developed technology has produced sandwich beam and plate structures in which the rubber materials are bonded between elastic materials as passive damping devices. Carbon black (CB) and silicon (Sil) are among the most popular fillers for industrial products. Our current goal is to be able to model the stress-strain relationships from quasi-static uniaxial strain tests on CB filled and Sil filled rubber rods. In the near future, we hope to incorporate results obtained here into a project on laminate (sandwich) beam structures that employ both piezo-ceramic patches and viscoelastic materials as active and passive control devices and to a project on "smart" rubber materials that contain additional particles that are piezoelectric and/or electromagnetic (see [13] and [16]). Complete constitutive laws of motion (dynamic) for the structures require accurate modeling of rubber characteristics such as viscoelasticity, large strain and hysteresis. To extend our current research to the sandwich beam structures, we will use results from [1], [2], [5] and [3] for setting up the mathematical framework. The first three references contain beam models that included the Boltzmann superposition integral in the stress-strain relationship, while the latter reference studies a general hyperbolic partial differential equation that includes a nonlinear constitutive operator. For the study of rubber materials that are filled with active particles, we will eventually require nonlinear homogenization techniques. Ultimately, with experimentally verified static and (uncontrolled) dynamic models, we hope to develop control laws for these projects. Thus, this research is one step in the effort of modeling "smart" elastomeric structures that are a class of active and passive control devices.

In the subsequent sections, we will outline some details of our investigations. The theoretical and experimental discussions are based on our joint efforts with scientists and engineers at Lord Corporation.

2 Models

A huge literature on modeling of viscoelastics and rubbers currently exists (e.g., [6]-[8],[10], [18], among the many discussed in [19]). In this section, we briefly mention existing linear and nonlinear models for stress-strain relationships in viscoelastic materials. Two categories of models can be found in the literature. One type is developed on the basis of the mechanical behavior of the samples, while the other concentrates on the microscopic behavior of the fibers, such as the changes in the cross linking of fibers and the contour length of fibers, and on the different relaxation times of fibers. Some of the models are in differential equation form, and the others are in integral form. The most fundamental integral model is the Boltzmann integral model, which captures the viscosity of the material and the history dependence of the stress on the strain and/or strain rate; the latter characteristic is a signature of the rubber materials. As is well known, the Boltzmann integral can be easily reduced to some well-known differential models, e.g., Kelvin-Voigt and Maxwell. Due to the fundamental importance of the Boltzmann integral, we digress here to outline its foundation.

2.1 Linear Models

The major assumption (a principle of superposition) made by Boltzmann is that linear models can be algebraically added together to generate more complicated models (see [14]). This assumption is referred to as the Boltzmann Superposition Principle (see [9], P. 6).

One can generalize the basic Kelvin-Voigt and Maxwell models (see [19], Chap. 3 for a detailed discussion) to relate the stress-strain by

$$\varepsilon(t) = \sigma_0 J(t)[H(t)] \text{ where } \sigma = \sigma_0[\mathrm{H(t)}] \tag{2.1}$$

$$\sigma(t) = \varepsilon_0 Y(t)[H(t)] \text{ where } \varepsilon = \varepsilon_0[\mathrm{H(t)}] \tag{2.2}$$

for functions $J(t)$ and $Y(t)$ that are termed the creep compliance function and the relaxation modulus function, respectively. Here H is the usual Heaviside function. Boltzmann generalized the above models to account for variables $\sigma(t)$ and $\varepsilon(t)$ (e.g., the the results from stretch and relaxation tests) by considering a succession of infinitesimal steps $d\varepsilon(t)$ for (2.1) or a succession of infinitesimal steps $d\sigma(t)$ for (2.2).

As a result, we obtain

$$d\sigma(t) = d\varepsilon(t')Y(t-t')[H(t-t')] \ . \tag{2.3}$$

We rewrite $d\varepsilon(t') = \frac{d\varepsilon(t')}{dt'}dt' \approx \frac{\partial\varepsilon(t')}{\partial t'}dt'$, set $t \geq t'$, and integrate (2.3) from 0^- to t to obtain

$$\sigma(t) = \int_{0^-}^{t} Y(t-t')\frac{\partial\varepsilon(t')}{\partial t'}dt' \ .$$

Similarly,

$$\varepsilon(t) \quad = \quad \int_{0^-}^{t} J(t-t')\frac{\partial \sigma(t')}{\partial t'}dt'$$

can be obtained. The above integrals are referred to as the Boltzmann integrals since they conform with the fundamentals of superposition as enunciated by Boltzmann. Physical models that consist of an infinite number of springs and dashpots are often associated with these integrals since they imply "adding" an infinite number of Maxwell and Kelvin-Voigt models together (see [9], [19]).

2.2 Nonlinear models

Typical nonlinear behaviors of the stress and strain in rubber materials under finite (i.e., non infinitesimal) deformation include a continuous increase of strain at decreasing rates upon loading, variable magnitudes of the strain subject to rates of loading, and different loading and unloading paths due to hysteretic memory effects. In addition, there are other nonlinear features that are particular to the samples under study. These traits can be modeled accurately to some degree using theories for finite deformations alone; however, to fully describe nonlinear viscoelastic material, it is desirable to also consider internal chemical and physical interactions involving long chain molecules and fillers. We refer the reader to [12] for the derivations of internal variable models and internal solid models, which are based on the molecular point of view. The previously mentioned Kelvin-Voigt model, Maxwell model and Boltzmann integral formulation can be modified to include finite deformations by making material coefficients functions of $\varepsilon(t)$ and t, or by defining new laws between $\sigma(t)$ and $\varepsilon(t)$. There are a number of models that involve attempts to model nonlinearity in viscoelastic material through finite deformation theories (see [9], [12], [17]). For more complete discussions we refer readers to Chapter 3 of [19] and a lengthy list of references found there.

Many of the various models in the literature have been verified qualitatively and/or numerically for certain samples under individual tests. However, due to the complex dependence of rubber materials on many physical parameters, it has been very difficult to obtain a general formulation that is reasonably simple quantitatively and that captures viscoelastic behavior across a wide range of materials. For our investigations here, we have used a Boltzmann law with nonlinear strain functional.

3 Theoretical Foundations

We consider simple extension in a rod of cross-sectional area A_c, length ℓ, mass density ρ with applied force $f(t)$ at the end $x = \ell$. We assume a Boltzmann law of the form

$$\sigma(t) = C\varepsilon(t) + \int_0^t Y(t-s)\frac{d}{ds}\tilde{g}(\varepsilon(s))ds \ . \tag{3.1}$$

Let $u(t,x)$ denote the displacement at time t of the section of the rod originally located at x, $0 \leq x \leq \ell$. If we assume that the rod begins its motion at rest with possible deformation $\Delta(x)$ and fixed end at $x = 0$, for smooth motion we obtain the model

$$
\begin{aligned}
\rho A_c \tfrac{\partial^2 u}{\partial t^2} &= \tfrac{\partial}{\partial x}(EA_c \tfrac{\partial u}{\partial x} - A_c \textstyle\int_0^t K(t-s)\tilde{g}(\tfrac{\partial u}{\partial x}(s))ds) \\
& \qquad 0 < x < \ell \\
\Big(EA_c \tfrac{\partial u}{\partial x} - A_c \textstyle\int_0^t K(t-s)\tilde{g}(\tfrac{\partial u}{\partial x}(s))ds\Big)_{x=\ell} &= f(t) \\
u(t,0) = 0, \quad u(0,x) = \Delta(x), \quad \dot{u}(0,x) = 0 \ ,
\end{aligned}
\tag{3.2}
$$

where $K(t) = -\frac{\partial Y}{\partial t}(t)$. In general, this model should be written in variational form

$$
\rho A_c \ddot{u} - \frac{\partial}{\partial x}\left(EA_c \frac{\partial u}{\partial x} - A_c \int_0^t K(t-s)\tilde{g}(\frac{\partial u}{\partial x}(s))ds\right) = F(t) \tag{3.3}
$$

in $V^* = H_L^1(0,\ell)^*$, where $F(t) = f(t)\delta_\ell$ with δ_ℓ the Dirac operator at $x = \ell$, $H_L^1(0,\ell) = \{\phi \in H^1(0,\ell) : \phi(0) = 0\}$, and derivatives interpreted in the distributional sense. This is exactly the same form as (2.21) of [5] (i.e., the extensional component with $w = 0$ — see also (3.1) of [5] and (6)-(8) of [4]) with nonlinearity $\tilde{g}(\xi) = E\xi + g(\xi)$. Separating and considering the linear part only, we have

$$
\rho A_c \ddot{u} - \frac{\partial}{\partial x}(EA_c \frac{\partial u}{\partial x} - EA_c \int_0^t K(t-s)\frac{\partial u}{\partial x}(s)ds) = F(t) \ . \tag{3.4}
$$

Taking r sufficiently large ($r = \infty$ is permissible if one does not wish to truncate at finite memory) and defining the shifted "history" variable $\gamma(t,s) = u(t) - u(t+s)$, $-r < s \le 0$, (see [1],[2],[5] for details) we obtain the equivalent equation

$$
\begin{aligned}
\rho A_c \ddot{u} &= \tfrac{\partial}{\partial x}\Big([E - E\textstyle\int_{-r}^0 K(-s)ds]A_c \tfrac{\partial u}{\partial x} \\
&+ \ EA_c \textstyle\int_{-r}^0 K(-s)\tfrac{\partial}{\partial x}\gamma(t,s)ds\Big) + F(t).
\end{aligned}
\tag{3.5}
$$

Following an approach we have used in earlier treatments of Boltzmann or time hysteresis stress-strain laws [1], [2], [5], we may write our model as an abstract system in a Hilbert space. Let $H = L^2(0,\ell)$ and $W = L_K^2(-r,0;V)$ with inner product

$$
\langle \eta_1, \eta_2 \rangle_W = \int_{-r}^0 K(-s)EA_c \langle \eta_1(s), \eta_2(s)\rangle_V \, ds \ .
$$

We define operators $\hat{\mathcal{A}} : V \to V^*, \mathcal{K} : W \to V^*$ by

$$
\begin{aligned}
\hat{\mathcal{A}}\phi &= -\frac{\partial}{\partial x}([E - E\int_{-r}^0 K(-s)ds]A_c \frac{\partial}{\partial x}\phi) \\
\mathcal{K}\eta &= \frac{\partial}{\partial x}(EA_c \int_{-r}^0 K(-s)\frac{\partial}{\partial x}\eta(s)ds) \ .
\end{aligned}
$$

Then our equation can be written

$$
\begin{aligned}
\rho A_c \ddot{u} &= -\hat{\mathcal{A}}u + \mathcal{K}\gamma + F \\
\dot{\gamma} &= \dot{u} + D\gamma
\end{aligned}
\tag{3.6}
$$

where $D = \frac{\partial}{\partial s}$ is defined on $domD \equiv \{\gamma \in H^1(-r,0;V) : \gamma(0) = 0\}$ into W. As a first order system on the state space $Z = V \times H \times W$, we finally have

$$\mathcal{M}\dot{z} = \mathcal{A}z + \mathcal{F} \tag{3.7}$$

for $z = (u, \dot{u}, \gamma)^T$, $\mathcal{F} = (0, F, 0)^T$, $\mathcal{M} = diag(I, \rho A_c, I)$ and

$$\mathcal{A} = \begin{pmatrix} 0 & I & 0 \\ -\hat{\mathcal{A}} & 0 & \mathcal{K} \\ 0 & I & D \end{pmatrix}$$

on $dom\mathcal{A} = \{(\phi, \psi, \eta) \in Z) | \psi \in V, \eta \in domD, -\hat{\mathcal{A}}\phi + \mathcal{K}\eta \in H\}$. Then arguments in Section 3 of [5] reveal that $\mathcal{A}$ is the infinitesimal generator of a strongly continuous semigroup $S(t)$ on Z. In that reference one also finds a development of computational techniques (finite elements) with convergence results in the context of a general approximation framework. We can use this to define (implicitly) mild solutions for our original nonlinear system (3.2) or (3.3) in terms of a nonlinear variation-of-parameters representation

$$z(t) = S(t)z(0) + \int_0^t S(t-\xi)[\mathcal{N}^*\mathcal{G}\mathcal{N}z(\xi) + \mathcal{F}(\xi)]d\xi \tag{3.8}$$

for appropriately defined operators $\mathcal{N}$ and $\mathcal{G}$. The details of well-posedness and convergence of approximation schemes for this nonlinear system as a perturbation of the basic linear system will be given elsewhere.

In our work reported on below, we have concentrated on the quasi-static case ($\ddot{u} = 0, \dot{u} \neq 0$) and attempted to identify the hysteresis kernel K and the nonlinearity g from experimental data. Before we turn to those results, a brief discussion of the philosophy of our approach in the context of other efforts is in order.

We may correctly view the Boltzmann representation approach as the introduction of internal dynamics into the viscoelastic system. To see this, let $\hat{\sigma} = (\sigma, \dot{\sigma}, \ddot{\sigma}, \cdots, \sigma^{(n_1)}), \hat{\varepsilon} = (\varepsilon, \dot{\varepsilon}, \ddot{\varepsilon}, \cdots, \varepsilon^{(n_2)})$ where n_1 and n_2 are nonnegative integers. If we suppose internal dynamics represented by the vector system

$$\frac{d}{dt}\hat{\sigma} = A\hat{\sigma} + \hat{\mathcal{F}}(\hat{\varepsilon}) \ , \tag{3.9}$$

then we have from the variation-of-parameters representation (assume $\hat{\sigma}(0) = 0$)

$$\hat{\sigma}(t) = \int_0^t e^{A(t-\xi)}\hat{\mathcal{F}}(\hat{\varepsilon}(\xi))d\xi$$

or

$$\sigma(t) = \int_0^t \sum_{j=1}^{n_1} X_{1j}(t-\xi)\hat{\mathcal{F}}_j(\hat{\varepsilon}(\xi))d\xi \ ,$$

where $X(t) = e^{At}$ is the matrix impulse response solution.

Thus, rather than an attempt to identify the internal dynamics (represented by the matrix operator A), our attempts to identify the Boltzmann kernels are equivalent to attempts to identify the solution operator e^{At} for the internal dynamics. This can be contrasted with the popular GHM method (and others) in the engineering literature ([11], [15]) which posits an internal variable model $\ddot{\sigma} + b\dot{\sigma} + c\sigma = \alpha\ddot{\varepsilon} + \beta\dot{\varepsilon}$, or in the frequency domain, $h(s) = (\alpha s^2 + \beta s)/(s^2 + bs + c)$, and attempts to identify the coefficients b, c, α, β from frequency data.

Those and other methods introduce extra variables to treat these internal dynamics and these variables also appear in the finite element realizations. This approach is similar in spirit to the methods of [1], [2], [5] where the extra hysteresis variable (called γ in (3.5) above) is used to account for the hysteretic phenomena (due to internal dynamics). In the engineering methods, the order of the internal dynamics is approximated early-on (by a ratio of finite polynomials) whereas in our approach, the history variable is infinite dimensional and is later approximated by high order (or low order if one wishes) finite element components (in the spaces $W^{M,N}$ of [5]). Of course, another fundamental difference in philosophy resides in whether one attempts to estimate A (the coefficients b, c, α, β of GHM) or the solution operator e^{At} (our Boltzmann kernel) for the internal dynamics.

4 Experimental Protocol Results

In a series of experiments at Lord Corporation, we tested filled rubber rods in simple uniaxial tensile deformations. Both ends of the rods were manufactured with metal flanges to be secured in a test machine, the Instron machine, which has a movable load cell that can apply tension to one end of the rods while keeping the other end fixed. The software package STD4200 was used to drive the Instron machine and to produce load-displacement curves upon stretching and relaxing the samples. If we denote the loading force by $f(t)$, the displacement by $\Delta\ell(t)$, the original length of the rod by ℓ, and the original area of the rod by A_c, then we calculate the engineering stress $\sigma(t) = \frac{f(t)}{A_c}$ and the strain $\varepsilon(t) = \frac{\Delta\ell(t)}{\ell} \times 100\%$. Two types of sample rods were used: ones filled with carbon black (CB) and ones filled with silicon (Sil). Quasi-static ($\ddot{u} = 0, \dot{u} = 5$ in/min) stretching/relaxation tensile cycles were performed on samples.

For each percent strain, the sample undergoes three cycles of stretching and relaxing to remove possible small scale Mullin's effects; this results in stress softening (see Figure 4.1). Note that the first cycle has higher values for the loads than the second and third loops. (Mullin's effect is very significant at the initial pulls on the sample. In fact, the CB filled sample was first pulled to approximately 300% strain and the Sil filled sample was pulled to 150% strain before we recorded data for lower percent strains.) We used the third cycle for each percent strain for our parameter estimation problems in the results presented in this note.

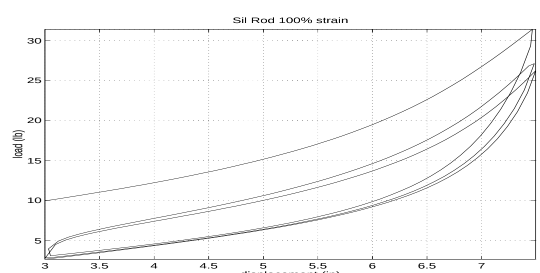

Figure 4.1: **Mullin's effect**

We report here on results for a CB rod ($\ell = 6.13$ in, diameter = .54 in after removal of Mullin's effects) and a Sil rod ($\ell = 7.455$ in, diam = .505 in). Assuming $\varepsilon(0) = 0$ for the rubber rods that are the focus of our studies, we used the following stress-strain relationship

$$\begin{aligned}\sigma(t) &= c_1\varepsilon(t) + \int_0^t Y(t-s)\frac{\partial g(\varepsilon(s))}{\partial s}ds \\ &= c_1\varepsilon(t) + Y(0)g(\varepsilon(t)) \\ &+ \int_0^t \frac{\partial Y(t-s)}{\partial t} g(\varepsilon(s))ds \end{aligned} \tag{4.1}$$

where $Y(t-s)$ is the memory kernel, $g(\varepsilon(s))$ is the nonlinear strain function and c_1 is an arbitrary constant that reduces to the Young's modulus in the linear elasticity range. This model conveniently provides a starting point for modeling the hysteresis curves, and it follows the same philosophy used in some of the well-studied models mentioned above. The challenge is to identify plausible memory kernels and finite strain expressions. We have investigated the kernels $Y(t) = c_2\varepsilon^{-c_3 t}$, $Y(t) = -c_2t^2+c_3t$, and $Y(t) = c_2t+c_3/(t+T)$ for positive constants c_2 and c_3 and for some final time T. We chose the exponential kernel since for a sequence of decreasing percent strains, it generated totally nested hysteresis loops, a feature that we also observed from our experimental data. We estimated the form of $g(\varepsilon(t))$ through stress data fitting, i.e., minimizing

$$\sum_{i=1}^{N} |\sigma(t_i) - \hat{\sigma}(t_i)|^2 \tag{4.2}$$

for stress data $\hat{\sigma}$. The MATLAB subroutine, *constr*, is used in this parameter estimation problem.

We tried a number of linear and nonlinear strain functions (see [19] for details). The relative errors discussed in [19] suggested that a nonlinear strain function $g(\varepsilon(t))$ is necessary for both the CB data and the Sil data for sufficiently large strains.

A second set of curve fitting involved using linear B-splines $\{B_i\}_{i=1}^N$ to approximate the load-displacement data. A force-balance equation ((3.2) with Dirac K, i.e., no hysteresis) can be used to describe either the stretch portion or the relaxation portion of our experiments

$$A_c g(\frac{\partial u(x)}{\partial x})|_\ell = f \tag{4.3}$$

where g is a nonlinear monotone function. If we assume $g^{-1}(x) = \sum_{i=1}^N a_i B_i(x)$, we can obtain a set of a_i that minimizes

$$|| \int_0^l g^{-1}(f/A_c)dx - \hat{u}||_2$$

where $\hat{u}$ is the displacement (either stretch or relaxation) data. We note that this model does not describe hysteresis, but it provides approximations to the nonlinearities in the least squares sense. This idea was also used in [4], in which similar experiments were carried out on different rods.

The preliminary estimation results were most useful (see [19]). These and other trials that involved using B-spline elements for the memory kernel suggested that a total of five to six undetermined coefficients (degrees of freedom) for the entire model (4.1) is needed to reach a certain level of accuracy. Since we found that each estimated g can be approximated by a cubic polynomial to within 1% of relative error, we chose $g = g(\epsilon(s), \dot{\epsilon}(s))$ given by

$$g(\varepsilon(s)) \quad = \quad \begin{cases} c_4\varepsilon(s) + c_5(\varepsilon(s))^2 + c_6(\varepsilon(s))^3 & \dot{\varepsilon}(s) > 0 \\ c_7\varepsilon(s) + c_8(\varepsilon(s))^2 + c_9(\varepsilon(s))^3 & \dot{\varepsilon}(s) < 0 \end{cases}$$

for our model. When we then estimated both the polynomial coefficients and exponential parameters (again least squares with (4.2)), we obtained the results in Figures 4.2 and 4.3. The results are satisfactory in terms of good approximations of the magnitudes of the variables and the shapes of the loops.

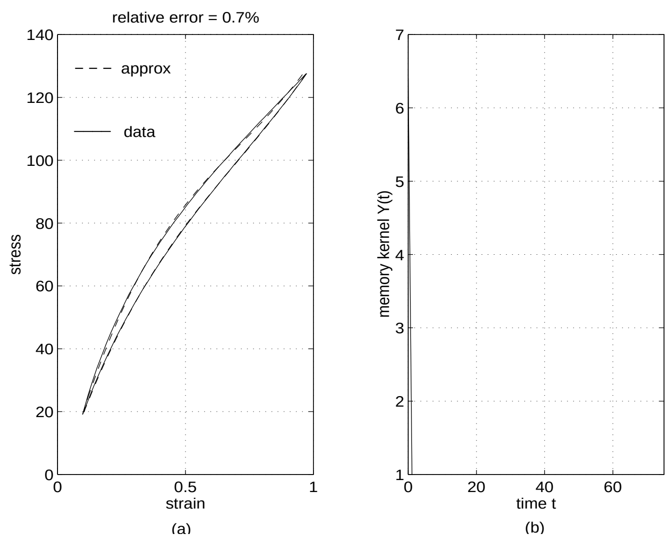

Figure 4.2: **CB rod: cubic nonlinearity, exponential kernel,** $c^* =$ **[526.6, 6.404, 3.312, 35.67, 34.77, - 18.74, 41.02, 23.91, - 13.20].**

We can report that over all the simulations, our model does a slightly better job fitting the (single) loops that are generated for the CB rod than those for the Sil rod. In summary, our model can capture the shapes of both types of loops, the loop with small area for the CB rod and the loop with large area for the Sil rod, and can approximate the data to an acceptable degree of accuracy.

4.1 Nested loops

Another desirable feature is for the model to predict nested loops with accuracy. To demonstrate capabilities we used only data from the outer loop (100% strain) to estimate nonlinearities and kernels. The resulting approximate model was then used to simulate the inner loops corresponding to 80% and 60% strain. The simulations involved consecutive 100% , 80% and 60% stretches and relaxations. Some preliminary findings are given in Figure 4.4 for a Sil rod. These results for the Sil rod are satisfactory with the predictive curves from the model following quite closely the experimental data.

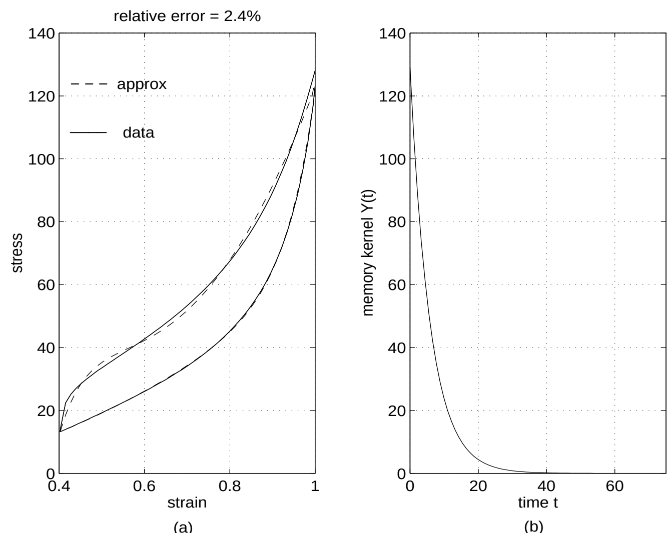

Figure 4.3: **Sil rod: cubic nonlinearity, exponential kernel,** $c^* =$ **[117.2, 129.1, 0.1694, 2.681, - 10.43, 15.21, - 0.4693, 3.780, - 1.5826]**

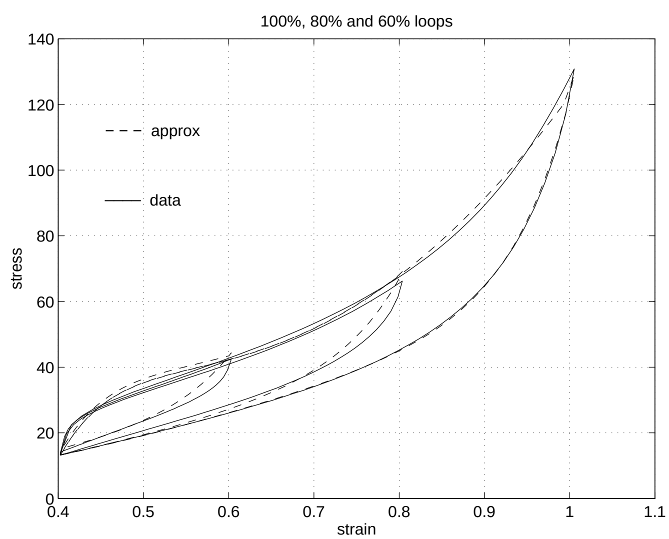

Figure 4.4: **Sil rod: Predicted loops, relative error = 5.6%**

5 Conclusion and Future work

In this note, we presented preliminary numerical findings using a generalized form of the Boltzmann integral to describe the stress-strain relationships for experiments done on carbon black filled and silicon filled rubber rods. These results suggest that our model is applicable; the hysteretic effects in these rubber rods are captured by the model. In future testing of the model, we will include it in dynamic partial differential systems for the vibration of filled rubber rods, sandwich beams and "smart" rubber structures.

6 Acknowledgment

We are grateful to M.J. Gaitens, B.C. Muñoz and L.C. Yanyo at Lord Corporation for their help on the actual experiments and on their insightful suggestions on the models.

This research was supported in part by the U.S. Air Force Office of Scientific Research under grants AFOSR F49620-95-1-0236, AFOSR F49620-95-1-0375, and in part by the U.S. Department of Education through a GAANN Fellowship to Y.Z. under grant P200A40730 and by an NSF-GRT fellowship to L.K.P. under grant GER-9454175.

References

[1] H.T. Banks, R.H. Fabiano and Y. Wang, *Estimation of Boltzmann damping coefficients in beam models*, Proceedings of COMCON Workshop on Stabilization of Flexible Structures, A.V. Balakrishnan and J.P. Zolesio, eds., Optimization Software Inc., New York, (1987), 13-35.

[2] H.T. Banks, R.H. Fabiano and Y. Wang, *Inverse problem techniques for beams with tip body and time hysteresis damping*, Mat. Aplic. e Comput. **8** (1989), 101-118.

[3] H.T. Banks, D.S. Gilliam and V.I. Shubov, *Gobal solvability for damped abstract nonlinear hyperbolic systems*, Differential and Integral Equations, **10** (1997), 309-332.

[4] H.T. Banks, N.J. Lybeck, M.J. Gaitens, B.C. Muñoz and L.C. Yanyo, *Computational methods for estimation in the modeling of nonlinear elastomers*, CRSC-TR95-40, Kybernetika, **32** (1996), 526–542.

[5] H.T. Banks, N.G. Medhin, and Y. Zhang, *A mathematical framework for curved active constrained layer structures: well-posedness and approximation*, CRSC-TR95-32, NCSU; Numerical Functional Analysis & Optimization, **17** (1996), 1-22.

[6] R. Bloch, W.V. Chang and N.W. Tschoegl, *The behavior of rubberlike materials in moderately large deformations*, Journal of Rheology, **22** (1978), 1-32.

[7] R. Bloch, W.V. Chang and N.W. Tschoegl, *On the theory of the viscoelastic behavior of soft polymers in moderately large deformations*, Rheologia Acta, **15** (1976), 367-378.

[8] R.M. Christensen, *Theory of Viscoelasticity: An Introduction*, 2nd ed., Academic Press, New York, 1982.

[9] W.N. Findley, J.S. Lai and K. Onaran, *Creep and Relaxation of Nonlinear Viscoelastic Materials*, H.A. Lauwerier and W.T. Koiter, eds., North-Holland Series in Applied Mathematics and Mechanics, North-Holland Publishing Company, 1976.

[10] J.D. Ferry, *Viscoelastic Properties of Polymers*, John Wiley & Sons, Inc., 1980.

[11] D.F. Golla and P.C. Hughes, *Dynamics of viscoelastic structures — A time-domain, finite element formulation*, ASME J. Applied Mechanics **52** (1985), 897-905.

[12] A.R. Johnson, C.J. Quigley and J.L. Mead, *Large strain viscoelastic constitutive models for rubber, part I: Formulations*, Rubber Chemistry Technology, **67** (1994), 904-917.

[13] M.R. Jolly, J.D. Carlson, B.C. Muñoz and T.A. Bullions, *The magnetoviscoelastic response of elastomer composites consisting of ferrous particles embedded in a polymer matrix*, Journal of Intelligent Material Systems and Structures **7** (1996), 613-622.

[14] H. Kolsky, *The measurement of the material damping of high polymers over ten decades of frequency and its interpretation*, V. K. Kinra and A. Wolfenden, eds., Mechanics and Mechanisms of Material Damping, American Society for Testing and Materials, Philadelphia, 1992.

[15] D.J. McTavish, P.C. Hughes, Y. Soucy and W.B. Graham, *Prediction and measurement of modal damping factors for viscoelastic space structures*, AIAA Journal **30** (1992), 1392-1399.

[16] B.C. Muñoz and M.R. Jolly, *Composites with field responsive rheology*, W.K. Brostow, ed., Performance of Plastics, Hansen Publisher, N.Y., 1997.

[17] A. Rivera-Dominguez and W.M. Jordan, *Predictive creep response of linear viscoelastic graphite/epoxy composites using the Laplace Transform method*, Journal of Materials Engineering and Performance, **1** (1992), 261-266.

[18] R.A. Schapery, *On the characterization of nonlinear viscoelastic materials*, Polymer Engineering and Science, **9** (1969), 295-310.

[19] Y. Zhang, *Mathematical formulation of vibrations of a composite curved beam structure: Aluminum core material with viscoelastic layers, constraining layers and piezoceramic patches*, Ph.D. Thesis, N.C. State University, May 1997.